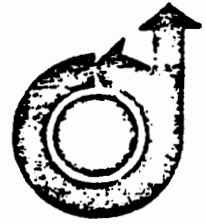


AIAA PAPER NO. 79-1695



**MAGNETOMETER BIAS DETERMINATION  
AND  
ATTITUDE DETERMINATION FOR  
NEAR-EARTH SPACECRAFT**

**GERALD M. LERNER  
AND**

**MALCOLM D. SHUSTER**

**Computer Sciences Corporation  
System Sciences Division  
Silver Spring, Maryland 20910**

**AIAA GUIDANCE AND CONTROL  
CONFERENCE**

**BOULDER, COLORADO  
AUGUST 6-8, 1979**

# MAGNETOMETER BIAS DETERMINATION AND ATTITUDE DETERMINATION FOR NEAR-EARTH SPACECRAFT<sup>1</sup>

G. M. Lerner\* and M. D. Shuster\*

Computer Sciences Corporation System Sciences Division  
Silver Spring, Maryland 20910

## Abstract

A simple linear-regression algorithm is used to determine simultaneously magnetometer biases, misalignments, and scale factor corrections, as well as the dependence of the measured magnetic field on magnetic control systems. This algorithm has been applied to data from the Seasat-1 and the Atmosphere Explorer Mission-1/Heat Capacity Mapping Mission (AEM-1/HCMC) spacecraft. Results show that complete inflight calibration as described here can improve significantly the accuracy of attitude solutions obtained from magnetometer measurements.

This report discusses the difficulties involved in obtaining attitude information from three-axis magnetometers, briefly derives the calibration algorithm, and presents numerical results for the Seasat-1 and AEM-1/HCMC spacecraft.

## Magnetometers As Attitude Sensors

Magnetometers are used widely for attitude determination and control. As part of an attitude control system, a three-axis magnetometer measures the strength and direction of the earth's magnetic field and can be used to compute electromagnetic torquing system commands to control the spacecraft angular momentum. Magnetic torquing can be used directly to control nutation, to precess the spacecraft angular momentum vector, or to maintain the speed of momentum wheels within prescribed limits.

For attitude control, a crude magnetometer will suffice. A commonly used momentum management control law<sup>1</sup> uses only the sign of the magnetic field vector components. In contrast, for attitude determination, the best magnetometers are inadequate when attitude accuracies better than 0.5 degree/axis are required.

The accuracy of attitude solutions from magnetometer measurements cannot exceed that of the magnetic field model. Errors in geomagnetic field models—e.g., IGRF75<sup>2</sup>—probably exceed 0.5 degree (3 $\sigma$ ) for a 600 to 800 km orbit. Even this attitude determination accuracy cannot be achieved without correction for numerous sources of additional error. These sources include bias magnetic fields produced in the spacecraft, internal misalignment or miscalibration of the magnetometer system, external misalignment of the magnetometer system relative to the spacecraft reference axes, and

calibration errors in the conversion of analog magnetometer measurements to digital telemetry data. Zero-mean error sources, such as noise on the analog signal and the finite size of the least-significant telemetered bit, also need to be considered.

Flight experience with magnetometers flown onboard SAS-1<sup>3</sup>, AE-3<sup>4</sup>, SAS-3<sup>5</sup>, AEM-1/HCMC<sup>6</sup>, and Seasat-1<sup>7</sup> has demonstrated the necessity of inflight calibration for attitude determination for spacecraft that use magnetometers for attitude control and thus incorporate magnetic torquing systems. On HCMC, an uncalibrated magnetometer was used to provide coarse (about 5-degree) attitude solutions during attitude acquisition, but has been of limited use in support of daily experimental operations.

This paper describes an algorithm for the inflight calibration of three-axis magnetometer systems. These methods have been applied to flight data for Seasat-1 and AEM-1/HCMC. Results show that inflight calibration like the type presented here can significantly improve attitude accuracy. For AEM-1/HCMC, the improvement is dramatic.

## Bias Determination Equations

The availability of a source of attitude knowledge independent of the magnetometer data is assumed. This source may be from any combination of star trackers, sun and earth sensors, or a dynamic model. The model chosen for bias determination is

$$A(t) \vec{B}_0(t) = (I + S) \vec{B}(t) + \vec{b} + T \vec{D}(t) \quad (1)$$

where  $A(t)$  = a 3 x 3 attitude matrix at time  $t$  that transforms vectors from reference to body coordinates. Since both spacecraft to be considered are earth-pointing, it will be convenient to choose orbital coordinates ( $\hat{z}$  = nadir,  $\hat{y}$  = negative orbit normal) as the reference system.

$\vec{B}_0(t)$  = the earth's magnetic field in reference (orbital) coordinates.

$\vec{B}(t)$  = the earth's magnetic field in the spacecraft body coordinates based on nominal (preflight) calibration of the magnetometer.

<sup>1</sup>Work supported by the Attitude Determination and Control Section, Goddard Space Flight Center, National Aeronautics and Space Administration, under contract no. NAS 5-24300

\*Member AIAA

$\vec{D}(t)$  = a telemetered control vector (e.g., the spacecraft control magnetic dipole), which is assumed to affect the magnetometer data linearly.

$\vec{b}$  = a bias vector, to be determined.

S = a 3 x 3 scale-factor/misalignment matrix, to be determined.

T = a 3 x 3 matrix relating the control vector to the magnetometer data, to be determined.

I = the 3 x 3 identity matrix.

The matrix I + S is the alignment/scale-factor matrix. If I + S is an orthogonal matrix, then the three magnetometer axes are orthonormal and coherently misaligned to the spacecraft reference axes. Non-zero diagonal elements of S are indicative of errors in the magnetometer axis scale factor--i.e., the constant relating magnetometer output to magnetic field. In general, the nine elements of S are small and unrelated and include both alignment and calibration errors.

The desired solutions for S, T, and  $\vec{b}$  are those which minimize the loss function

$$L = \sum_{i=1}^N a_i |\vec{H}_i - \vec{b} - S\vec{B}_i - T\vec{D}_i|^2 \quad (2)$$

where

$$\vec{H}_i = A(t_i) \vec{B}_o(t_i) - \vec{B}(t_i) \quad (3a)$$

$$\vec{B}_i = \vec{B}(t_i) \quad (3b)$$

$$\vec{D}_i = \vec{D}(t_i) \quad (3c)$$

and the  $a_i$  are nonnegative weights associated with the measurements at the time  $t_i$  and normalized so that

$$\sum_{i=1}^N a_i = 1 \quad (4)$$

Straightforward minimization of this loss function leads to the equations

$$S \langle \vec{B} | \vec{B} \rangle + T \langle \vec{D} | \vec{B} \rangle = \langle \vec{H} | \vec{B} \rangle \quad (5a)$$

$$S \langle \vec{B} | \vec{D} \rangle + T \langle \vec{D} | \vec{D} \rangle = \langle \vec{H} | \vec{D} \rangle \quad (5b)$$

$$\vec{b} = \langle \vec{H} \rangle - S \langle \vec{B} \rangle - T \langle \vec{D} \rangle \quad (5c)$$

where the mean of a vector has been written as

$$\langle \vec{F} \rangle = \sum_{i=1}^N a_i \vec{F}_i \quad (6)$$

and the covariance matrix of two vectors as

$$\langle \vec{F} | \vec{G} \rangle = \langle \vec{F} \vec{G}^T \rangle - \langle \vec{F} \rangle \langle \vec{G} \rangle^T \quad (7)$$

Equations (5a) and (5b) may be reduced further to obtain

$$S = [\langle \vec{H} | \vec{B} \rangle - \langle \vec{H} | \vec{D} \rangle \langle \vec{D} | \vec{D} \rangle^{-1} \langle \vec{D} | \vec{B} \rangle] \cdot [\langle \vec{B} | \vec{B} \rangle - \langle \vec{B} | \vec{D} \rangle \langle \vec{D} | \vec{D} \rangle^{-1} \langle \vec{D} | \vec{B} \rangle]^{-1} \quad (8)$$

and an identical expression for T with  $\vec{B}$  and  $\vec{D}$  interchanged. When the term linear in the control vector is not included in the loss function, the simpler result is obtained

$$S = \langle \vec{H} | \vec{B} \rangle \langle \vec{B} | \vec{B} \rangle^{-1} \quad (9a)$$

$$\vec{b} = \langle \vec{H} \rangle - S \langle \vec{B} \rangle \quad (9b)$$

#### Application To Seasat-1

#### Calibration Results

Four orbits of Seasat-1 data (325 samples) were analyzed. Reference attitudes were computed using data from an Adcole sun sensor and an ITHACO infrared horizon scanner, which provided an attitude accuracy of 0.3 degree/axis (3 $\sigma$ ). The results for the magnetometer misalignment/scale-factor matrix and the bias vector are given in Table 1.

Table 1 Inflight Calibration of the Seasat-1 Magnetometer

PARAMETER	DATA DAYS ANALYZED						
	205	219	225	227	228	229	231
S <sub>11</sub>	018	0097	021	0184	0207	0200	0211
S <sub>12</sub>	008	0780	048	0204	0178	0211	0164
S <sub>13</sub>	007	0027	063	0048	0082	0040	0041
S <sub>21</sub>	013	0046	016	0077	0126	0140	0127
S <sub>22</sub>	048	1148	082	0082	0228	0318	0216
S <sub>23</sub>	007	0027	009	0028	0047	0028	0027
S <sub>31</sub>	002	0190	006	0089	0032	0088	0049
S <sub>32</sub>	019	1988	037	1081	0037	0126	0028
S <sub>33</sub>	001	0018	002	0038	0018	0022	0021
b <sub>1</sub> mG	72.5	89.7	78.1	72.3	71.4	71.1	71.5
b <sub>2</sub> mG	-28.6	26.1	22.8	28.5	28.5	28.4	28.1
b <sub>3</sub> mG	81.4	65.1	63.2	58.6	67.2	62.8	61.2
NOISE mG	3.2	3.8	3.2	3.1	3.3	3.7	3.7
SAMPLES	92	88	101	44	193	210	125

The exclusion of a term linear in the control vector is justified in the case of Seasat-1, since the control electromagnets are separated from the magnetometers by 6 m. Thus, a control magnetic dipole of 10<sup>5</sup> pole-cm can create a magnetic field of magnetic no greater than 1.7 mG at the magnetometers.

Data from 4 days were analyzed: Day 205 (July 24, 1978), Day 219 (August 7), Day 225 (August 13), and Day 227 (August 15). For the first 3 days,  $\vec{H}_1$  and  $\vec{E}_1$  were obtained every minute for approximately one orbit (100 minutes); for Day 227, only 44 minutes of data were available. The four orbits were analyzed individually, as shown in the first four columns of Table 1, and combined to provide data bases containing 193, 210, and 325 samples. The largest data base consisted of  $3 \times 325 = 975$  magnetic field components.

The data indicates that the bias vector,  $\vec{b}$ , is well defined, independent of the size of the data base, and that the magnitude of  $\vec{b}$ , 98.2 mG, is about 40 percent of the earth's field at the Equator (for Seasat at 800 km). The reason for this large bias is unclear; however, it is clear that attitudes computed from Seasat magnetometers data are useless without inflight calibration. The matrix S is not observable using data from a single orbit, although the larger samples give reasonably consistent results for all the components except  $S_{32}$ . The diagonal components of S,  $S_{11} = 0.021$ ,  $S_{22} = -0.022$ , and  $S_{33} = 0.002$ , indicate scale factor calibration errors for the X- and Y-axes of up to 2 percent. The off-diagonal elements of S, the largest of which is  $S_{12} = -0.016$ , are equivalent to alignment errors of up to 1 degree. The elements of S are consistent with values expected from the specified alignment and calibration accuracy. Because S is not skew-symmetric, the misalignment of the vector magnetometer relative to the body reference axes is not a simple rotation. Rather, S contains information on internal alignment, external alignment, and crosstalk.\* These cannot be separated.

The quality of the fit of 12 parameters to as many as 975 data items may be judged by the root-mean-square (rms) deviation between the modeled and measured field components. Table 2 lists the various sources of error which contribute to the observed rms error of 3.7 mG. The known error is 2.6 mG, implying an unknown error of  $\sqrt{(3.7)^2 - (2.6)^2} = 2.6$  mG. This unknown error could include such sources as noise on the analog magnetometer output, undetected bit errors, and currents associated with the power subsystem (the solar arrays and power cables are located near the magnetometer). Note that for GEOS-3 in a similar orbit, the rms error was 1.5 mG, of which all but 1.0 mG resulted from the least significant bit (lsb) size<sup>11</sup>.

#### Seasat Yaw Determination Accuracy

The magnetometers may be used to measure yaw angle during orbit night and the portion of the orbit when the sun is not visible to any of the four sun sensors. During the last half of August 1978 and during September 1978, sun sensor data were available only in the Southern Hemisphere for about 20 percent of the orbit (30 to 35 percent of the orbit was in darkness) and magnetometer data were needed to supplement interpolation

\*Crosstalk refers to induced magnetic fields normal to an applied field caused by ferromagnetic material and associated electronics.

\*\*Caused by a massive, progressive short circuit in the slip ring assembly drawing power from one of the two solar arrays.

methods for yaw determination<sup>12</sup>. Because of the Seasat spacecraft's failure on October 10, 1978,\*\* after a 106-day mission, it is particularly important to provide the best possible yaw angle data during that short period.

Table 2 Sources of Unmodeled Error for Seasat

SOURCE	MAGNITUDE	CONTRIBUTION TO RMS ERROR	REFERENCE
MAGNETOMETER LEAST SIGNIFICANT BIT	4.4 mG	1.3 mG	8
REFERENCE ATTITUDE ERROR	0.1 degree	0.5 mG	9
ELECTROMAGNET ACTIVITY	$10^5$ pole cm (3 axes)	1.7 mG	THIS WORK
FIELD MODEL ERROR	IGRF85	1.4 mG	10
ANTICIPATED RMS ERROR		2.6 mG	-

To first order in the attitude angles, yaw may be expressed as a function of the magnetometer data and known roll and pitch angles as

$$y = \frac{B_{02}(B_1 + pB_3) - B_{01}(B_2 - rB_3)}{B_{01}^2 + B_{02}^2} \quad (10)$$

where  $\vec{B}$  is the measured magnetic field in the body after inflight calibration and  $\vec{B}_0$  is the magnetic field in orbital (reference) coordinates. The quantities y, r, and p (yaw, roll, and pitch) are a 3-1-2 set of Euler rotation angles from orbital to body coordinates.

The expected yaw variance,  $\sigma_y^2$ , may be written as a function of the variance of the magnetometer measurements,  $\sigma_B^2$ , and the variance in the Euler angles,  $\sigma_\theta^2$ , assumed to be the same for pitch and roll. The result is

$$\sigma_y^2 = \frac{\sigma_B^2 + B_{03}^2 \sigma_\theta^2}{B_{01}^2 + B_{02}^2} \quad (11)$$

For the Seasat orbit (inclination = 108 degrees, eccentricity = 0., semi-major axis = 7168 km), the yaw variance is a minimum at the equator, where the standard deviation has the value

$$\sigma_y \Big|_{\text{equator}} = 0.92 \text{ degree} \quad (12)$$

The maximum yaw error occurs near the magnetic poles, where the denominator of Equation (10) vanishes. For

the data base used in computing the biases above, the largest yaw error was

$$\sigma_y \Big|_{\text{pole}} = 11 \text{ degrees} \quad (13)$$

In addition, one must consider the error associated with the size of the least significant bit (lsb) in the magnetometer telemetry, which is equivalent to 4.4 mG. This leads to yaw angle quantization errors from 0.4 degree (from X-axis quantization) to 1.0 degree (from Y-axis quantization) at the Equator, and correspondingly larger errors at the poles. In principle, lsb errors have zero mean and can be removed by filtering or smoothing of yaw solutions. In practice, however, the

lsb size is an important source of systematic yaw error because the magnetometer measurements change slowly at the orbit rate.

Figure 1 shows a comparison of yaw angle solutions computed using horizon scanner data and either sun sensor data or magnetometer data. The sun sensor yaw solutions are believed to be accurate to  $\pm 0.3$  degree; the magnetometer yaw solutions were computed using mean biases over the orbit,  $T = S = 0$ ,  $\vec{b} = (69.3, -30.3, -61.9)^T$  mG, and averaged over 120-second intervals to reduce the effects of magnetometer data digitization and noise. The figure indicates that, when mean biases are used, the magnetometer yaw solutions are worse than the

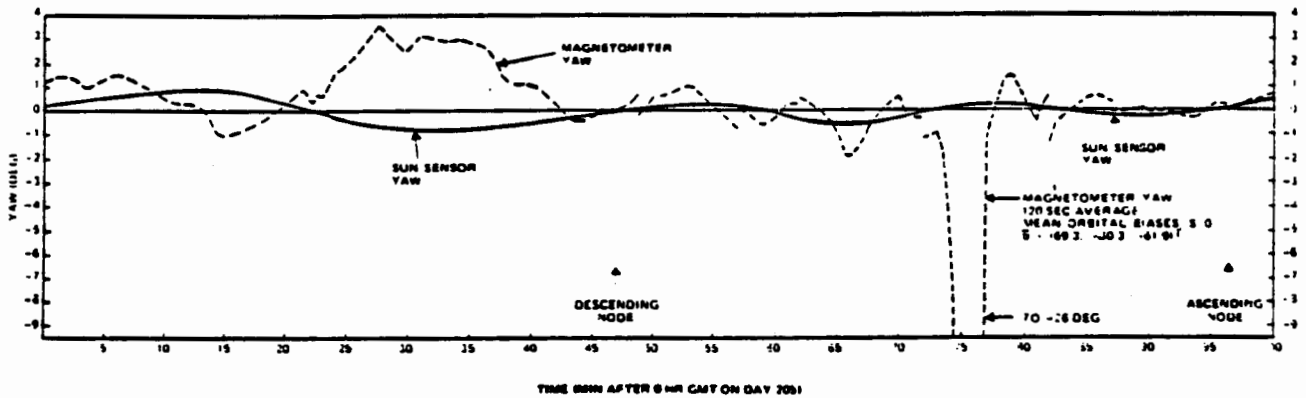


Fig. 1 Comparison of Sun Sensor and Magnetometer Yaw Angle Solutions for Day 205 Using Mean Bias for the Orbit

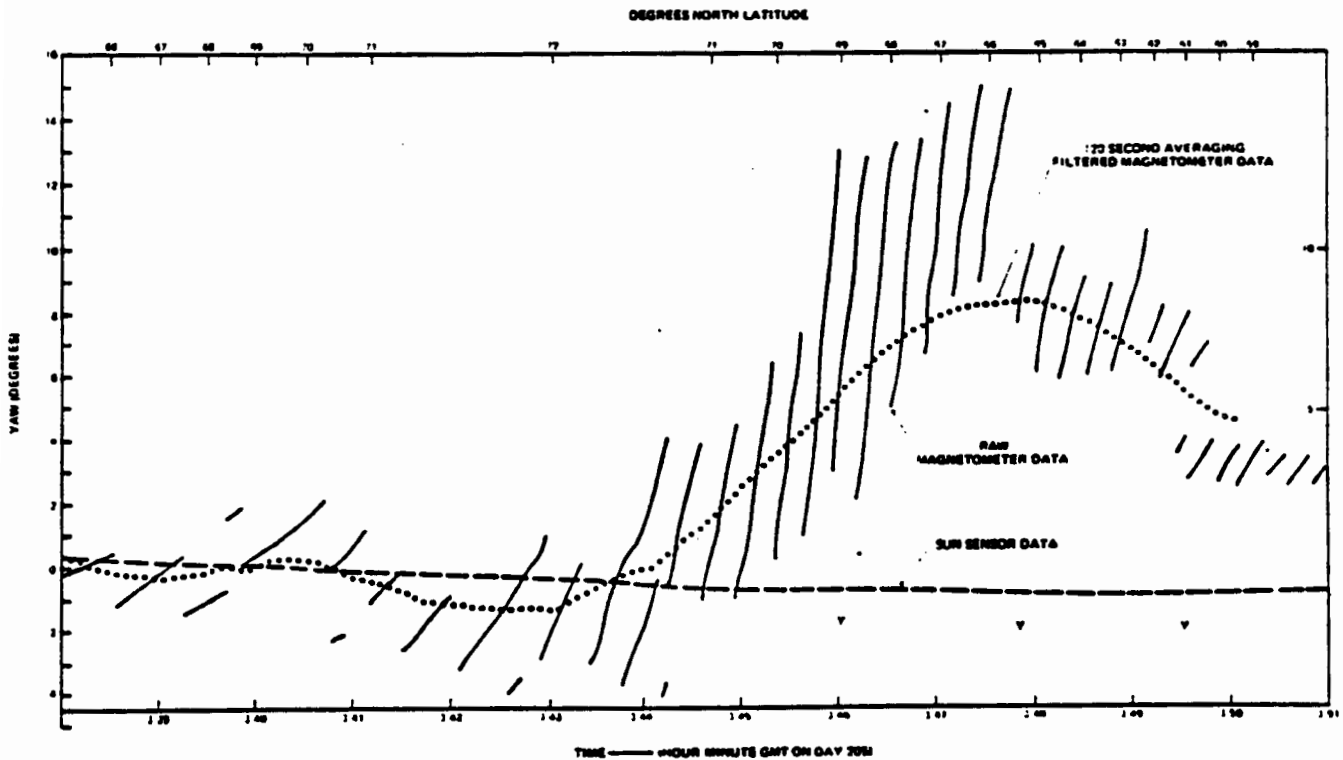


Fig. 2 Comparison of Yaw Solutions Using Sun Sensor and Magnetometer Data (1 of 3)

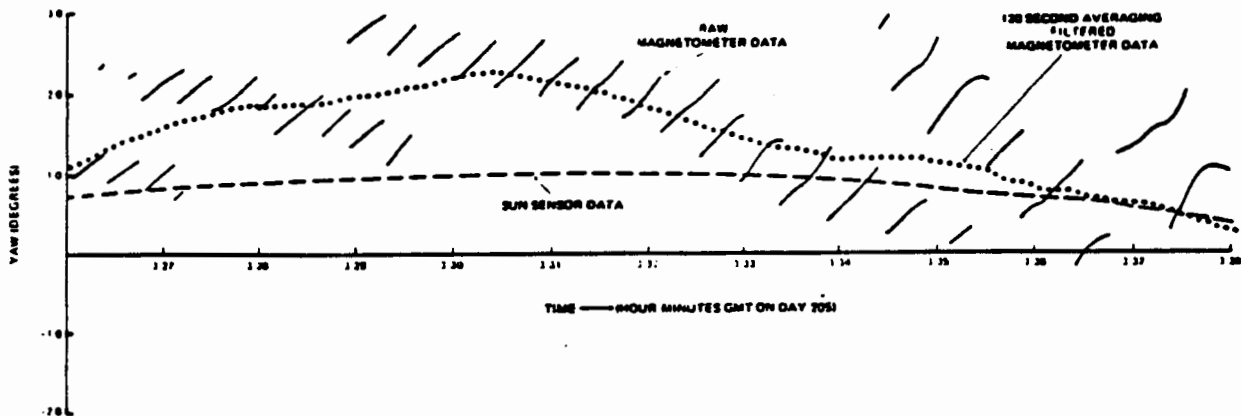


Fig. 2 Comparison of Yaw Solutions Using Sun Sensor and Magnetometer Data (2 of 3)

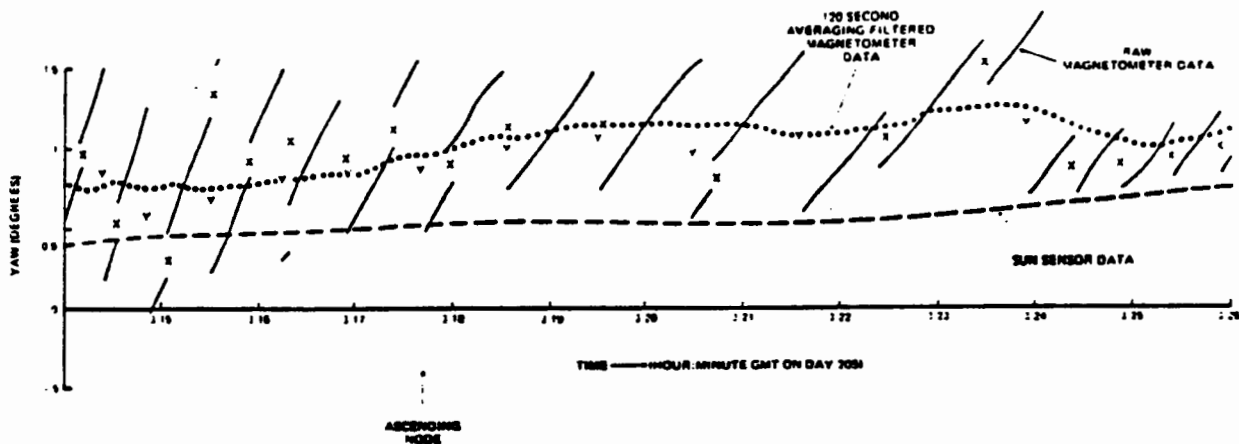


Fig. 2 Comparison of Yaw Solutions Using Sun Sensor and Magnetometer Data (3 of 3)

trivial solution yaw = 0 over the entire orbit, even near the ascending and descending nodes where the errors should be the smallest.

Figure 2 shows a comparison of the sun sensor and magnetometer yaw solutions using the inflight calibration parameters given in the last column of Table 1. In the figure, the dashed line indicates the sun sensor solution, the broken lines denote individual magnetometer solutions with the X- or Y-axis magnetometer bit changes indicated by the symbols X or Y, and the dotted line is the magnetometer yaw solution obtained by averaging over 120-second intervals. The figure shows that the inflight calibration substantially improves the accuracy of the magnetometer solutions, although the solution yaw = 0 is still the better estimate over most of the orbit. The yaw angle accuracy and the yaw angle lsb in Figure 2 are in good agreement with the estimates presented earlier. Data from Day 279 were used to verify that the calibration parameters computed using data from Days 205, 219, 225, and 227 are valid for other days. The rms magnetometer data residuals for 125 minutes

were 2.2, 4.2, and 1.7 mG. for the X-, Y-, and Z-axis, respectively. Because of the limited sun sensor data coverage on Day 279, the data are either from sun sensor 2, south of 45 degrees south Latitude, or from sun sensor 3, north of 30 degrees north Latitude. This data selection, corresponding to regions of the earth where the field is primarily along the yaw axis and the sun is near the horizon, is probably responsible for the large Y-axis residual and the small X- and Z-axis residuals. The small overall rms residual,  $[(2.2)^2 + (4.2)^2 + (1.7)^2]^{1/2} = 2.9$  mG, does, however, indicate that the magnetometer calibration is valid.

#### Application To AEM-1/HCMM

##### Calibration Results

The HCMM mission is described in Reference 13. The attitude determination hardware consists of an infrared earth horizon sensor, three two-axis sun sensors, and a three-axis fluxgate magnetometer. The magnetometer is part of the magnetic attitude and momentum

control system and is located within a meter of three 10,000 pole-cm electromagnetic torquing coils. The proximity of the coils and magnetometers can result in a bias of approximately 20 mG, which is removed, in part, by electronic compensation. This compensation may be thought of as subtracting bias voltages, proportional to the dipole currents, from the magnetometer voltages. The compensation is desired to reduce the effective dipole bias to a value less than 1 mG. Thus, as in the case of Seasat-1, we assume that  $\bar{D}_1 = 0$ .

Magnetometer and sun sensor data were used to provide coarse attitude information during the early orbits of the mission. Subsequent to the initiation of normal experimental operations, however, magnetometer data were found to be of little use in meeting the experimenter's attitude accuracy requirements of 0.5 degree for pitch, 0.7 degree for roll, and 2.0 degrees for yaw<sup>6</sup>. This was because the HCMM software was capable of solving only for  $\bar{b}$  in Equation (2), under the assumption that  $S = T = 0$ . The values obtained for  $b$  varied from data pass to data pass by as much as  $\pm 10$  mG in the case of  $b_1$ .

Table 3 shows the results of the inflight calibration. It should be noted that the rms difference between the model field and the calibrated magnetometer is 2.2 mG, considerably smaller than the value of 3.7 mG obtained for Seasat-1. The smaller error was obtained despite a poorer attitude reference and greater electromagnetic effects. Table 4 lists the error sources for HCMM and shows that the observed rms residual may be accounted for fully by the known error sources. This result indicates that the electronic compensation works well for HCMM.

Table 3 Inflight Calibration of the HCMM Magnetometer

PARAMETER	DATA DAYS ANALYZED <sup>1</sup>		
	SET A	SET B	SETS A AND B
$s_{11}$	0.080	0.074	0.086
$s_{12}$	0.011	0.007	0.008
$s_{13}$	-0.003	-0.003	-0.003
$s_{21}$	-0.020	-0.017	-0.019
$s_{22}$	0.022	0.010	0.014
$s_{23}$	0.018	0.018	0.018
$s_{31}$	0.028	0.020	0.024
$s_{32}$	0	-0.008	-0.004
$s_{33}$	-0.007	-0.007	-0.007
$b_1$ (mG)	-9.7	-12.6	-11.1
$b_2$ (mG)	16.2	15.8	16.1
$b_3$ (mG)	-1.7	-0.9	-1.5
RMS (mG)	2.4	2.0	2.2
SAMPLES	132	308	443

<sup>1</sup>SET A - DAYS 285, 284, 287, AND 289

SET B - DAYS 279, 290, 292, 298, 300, AND 302

Table 4 Sources of Unmodeled Error for HCMM

SOURCE	MAGNITUDE	CONTRIBUTION TO RMS ERROR	REFERENCE
MAGNETOMETER LSB	4.7 mG	1.6 mG	13
REFERENCE ATTITUDE ERROR	2	1.1 mG	6
ELECTROMAGNET ACTIVITY	5	1 mG	13
FIELD MODEL ERROR	IGRF 75	10 TO 15 mG	2
MAGNETOMETER NOISE	NEGLIGIBLE		
ANTICIPATED TOTAL RMS ERROR		2.9 TO 2.5 mG	

<sup>4</sup>DURING SUNLIT PASSES, THE RMS PITCH AND ROLL ERROR ESTIMATES ARE 0.15 DEG AND 0.12 DEG RESPECTIVELY (REFERENCE 7). THE RMS YAW ERROR DURING SUNLIT PASSES IS ESTIMATED FROM FIGURE 4-94 TO 4-97 OF REFERENCE 1 AS 0.3 DEG

<sup>5</sup>ELECTRONIC COMPENSATION FOR LARGE (20 mG) MAGNETOMETER BIASES IS USED ON THE AEROSPACECRAFT. RESIDUAL EFFECTS ARE BELIEVED TO BE LESS THAN 1 mG

The parameters in Table 3 show that a 7 percent error in the X-axis scale factor is the main reason that the apparent X-axis bias varied from pass to pass and that the uncalibrated magnetometers could not provide useful attitude data. Misalignments of 1 to 1.4 degrees and X- and Y-axis biases of -11 and +16 mG also contributed to the magnetometer data problems.

The data in Table 5 illustrate the performance of the HCMM magnetometers, following the use of the calibration parameters listed in the last column of Table 3. Forty-three data segments were analyzed, each corresponding to a 2- to 12-minute pass over the Orroral Valley, Australia (ORR), Engineering Training Center, Maryland (ETC), Merrit Island, Florida (MIL), Goldstone, California (GDS), Winkfield, England (WNK), Madrid, Spain (MAD), or Fairbanks, Alaska (ULA) tracking station. This data base represents all the HCMM data transmitted from 14 hr GMT on November 29, 1978, to 0 hr GMT on December 2, 1978. It should be noted that HCMM, unlike Seasat, does not have tape recorders onboard; thus data are acquired only over the supporting tracking stations. The station names and acquisition of signal (AOS) times (GMT) are given in the first two columns of Table 5.

The accuracy of the calibrated magnetometer data may be judged by examining the scalar (i.e., attitude-independent) parameters in the table. The field model residual,

$$\epsilon_M = \left( \frac{1}{N} \sum_{i=1}^N [M_M(t_i) - M_C(t_i)]^2 \right)^{1/2} \quad (14)$$

is the rms difference between the measured field magnitude,  $M_M(t_i)$ , and the model field magnitude,  $M_C(t_i)$ , at time  $t_i$ . If the only source of error were the 4.7 mG lsb of the telemetered magnetometer data, the rms residual would be

$$\sigma_{\epsilon_M} = 4.71 / \sqrt{12} = 1.36 \text{ mG} \quad (15)$$

The third column of Table 5 shows that, for the data base,  $\epsilon_M$  ranges from 1.65 to 5.46 mG, and that, for

Table 5 HCMM Attitude Data Summary

AOS	STATION	FIELD MAGNITUDE RESIDUAL $\epsilon_M$ (MG)	SUN-FIELD ANGLE		NADIR-FIELD ANGLE		SUN-NADIR ANGLE	
			RANGE $\theta_{SM}$ (DEG)	RESIDUAL $\Delta\theta_{SM}$ (DEG)	RANGE $\theta_{EM}$ (DEG)	RESIDUAL $\Delta\theta_{EM}$ (DEG)	RANGE $\theta_{SE}$ (DEG)	RESIDUAL $\Delta\theta_{SE}$ (DEG)
781129.1400	ORR*	2.03	110-148	0.75*	146-162	0.33	55-77	0.67*
1535	ORR*	2.11	116-154	0.69*	138-163	0.41	47-73	0.82*
1801	ETC	2.75	108-154	0.32	17-31	0.37	100-131	0.24
1935	MIL	2.16	128-183	0.38	24-50	0.46	111-141	0.25
2116	GDS	2.08	122-166	0.35	18-31	0.38	105-131	0.21
781130.0053	WNK	2.14	-	-	44	0.82	28-47	-
0067	MAD	2.12	-	-	27-43	0.94	27-44	-
0229	WNK	2.15	-	-	10-15	0.88	28-30	-
0234	MAD	2.11	-	-	16-43	0.89	27-57	-
0324	ORR	1.84	36-52	0.29	133-162	0.32	137-153	0.16
0550	ETC	5.46	-	-	16-36	0.77	27-42	-
0725	ETC	3.38	-	-	9-11	0.58	27-48	-
0727	MIL	3.36	-	-	11-54	0.55	27-41	-
0904	GDS	1.79	-	-	16-46	0.44	27-42	-
1040	GDS	2.00	-	-	14-46	0.47	27-45	-
1153	MAD	2.01	114-158	0.37	17-35	0.42	97-124	0.26
1154	WNK	1.96	95-154	0.36	17-31	0.37	85-120	0.29
1326	MAD	2.24	114-155	0.34	41-46	0.39	99-135	0.22
1329	WNK	2.28	93-185	0.33	13-41	0.35	85-127	0.25
1348	ULA	1.78	-	-	6-24	0.36	40-64	-
1417	ORR*	1.96	110-149	0.72*	140-162	0.37	52-76	0.61*
1584	ORR*	2.43	121-155	0.65*	142-165	0.47	48-70	0.64*
1615	MIL	2.92	124-156	0.40	39-52	0.51	110-143	0.25
1619	ETC	2.71	104-156	0.37	12-39	0.40	98-132	0.27
2008	ULA	1.64	81-102	0.40	7-10	0.28	79-94	0.29
2132	GDS	2.22	118-167	0.32	19-48	0.36	102-136	0.22
2141	ULA	1.93	80-127	0.33	9-19	0.33	76-107	0.25
2318	ULA	2.09	85-133	0.30	10-25	0.33	79-108	0.26
781201.0111	WNK	2.31	-	-	14-18	0.69	27-57	-
0115	MAD	2.34	-	-	16-44	0.96	26-45	-
0247	WNK	2.33	-	-	10-13	0.73	28-61	-
0251	MAD	2.29	-	-	13-42	0.84	27-48	-
0342	ORR	1.74	35-62	0.27	134-164	0.34	138-154	0.18
0607	ETC	5.22	-	-	12-38	0.74	27-43	-
0743	ETC	2.85	-	-	10-15	0.81	27-48	-
0746	MIL	2.87	-	-	15-53	0.66	26-39	-
0821	GDS	1.66	-	-	14-46	0.44	26-44	-
1089	GDS	2.03	-	-	19-46	0.40	27-43	-
1347	WNK	2.16	99-154	0.37	10-41	0.32	89-127	0.25
1610	ORR*	2.34	128-155	0.75*	133-165	0.52	44-66	0.68*
1637	ETC	2.55	110-128	0.37	12-44	0.38	101-132	0.24
2014	GDS	2.00	115-165	0.33	16-43	0.32	102-134	0.24
2150	GDS	2.19	121-167	0.34	19-50	0.34	103-136	0.23
RMS VALUES		2.20		0.36		0.51		0.24
		(39 PASSES)		(39 PASSES)		(39 PASSES)		(19 PASSES)
		2.50				0.53		
		(43 PASSES)				(43 PASSES)		

\*DAWN PASS OVER ORRORAL. THESE PASSES ARE NOT USED IN THE COMPUTATION OF THE OVERALL RMS VALUES FOR  $\Delta\theta_{SM}$  OR  $\Delta\theta_{SE}$ . SEE TEXT FOR EXPLANATION.



all but four passes (ETC at 11/30 5 hr 50 min GMT, 11/30 7 hr 25 min GMT, 12/1 6 hr 7 min GMT and MIL at 11/30 7 hr 27 min GMT),  $\epsilon_M < 3\text{mG}$ . The remaining 39 passes have an unmodeled rms field residual of

$$\delta\epsilon_M = \left[ (2.2)^2 - \sigma_{\epsilon_M}^2 \right]^{1/2} = 1.7 \text{ mG} \quad (16)$$

which may be fully accounted for by errors in the field model and electromagnetic activity (see Table 4).

The origin of the unusually high field magnitude residual for the three passes between 5 hr 50 min GMT and 7 hr 27 min GMT on November 30 and the ETC pass at 6 hr 7 min GMT on December 1 is unknown. These passes all occurred at night over the region of primary experimental interest, so that bias fields produced by onboard hardware may be responsible.

Angular errors in the direction of the magnetic field may be estimated by

$$\delta\theta_M = \frac{\delta\epsilon_M}{M} \quad (17)$$

where M varies from 230 mG near the Equator to 460 mG near the poles. This implies an rms angular error in the range

$$0.42^\circ \leq \delta\theta_M \leq 0.21^\circ \quad (18)$$

with the larger errors near the Equator.\*

The angular errors also may be estimated from rms residuals of the form,

$$\Delta\theta_{XY} = \left\{ \frac{1}{N} \sum_{i=1}^N \left[ \cos^{-1} \left( \hat{X}_M(t_i) \cdot \hat{Y}_M(t_i) \right) - \cos^{-1} \left( \hat{X}_C(t_i) \cdot \hat{Y}_C(t_i) \right) \right]^2 \right\}^{1/2} \quad (19)$$

where  $\hat{X}$  and  $\hat{Y}$  denote the direction of any two of the field (M), sun (S), and nadir (N) reference vectors. The subscripts M and C denote the measured and computed values for these angles. As for  $\epsilon_M$ ,  $\Delta\theta_{XY}$  is composed of (zero-mean) noise and lsb errors in the measured field, sun, and nadir vector directions and systematic sensor errors. Errors in the sun and spacecraft ephemerides are negligibly small so that errors in  $\hat{M}_C$  contribute to errors in  $\Delta\theta_{SM}$  and  $\Delta\theta_{EM}$ , but not in  $\Delta\theta_{SE}$ .

which may be used to estimate errors in the measured sun,  $\hat{S}_M$ , and nadir,  $\hat{E}_M$ , vectors.

HCMM flies three two-axis sun sensor heads, sensors 1, 2, and 3, each with a 128-degree by 128-degree field-of-view and a 0.5 degree lsb (Reference 13). Sensors 2 and 3 were used to calibrate the horizon scanner data with an algorithm<sup>14</sup> that, in essence, assumes that the sun sensor orientation in the spacecraft is known and calibrates the scanner by minimizing  $\Delta\theta_{SE}$ . Thus, for purposes of attitude determination, sun sensors 2 and 3 and the horizon scanner define the HCMM attitude reference axes. Data from these three sensors are assumed to be free of systematic errors.

A malfunctioning sun sensor 1 provided no useful attitude data from launch (on April 26, 1978) until November 1978, when, during dawn over Orroral, the sun passed close to the center of the sensor field-of-view<sup>6</sup>. Five passes of Orroral data (on 11/29 at 14 hr 0 min GMT and 15 hr 35 min GMT, on 11/30 at 14 hr 17 min GMT and 15 hr 54 min GMT, and on 12/1 at 16 hr 10 min GMT) yield values of  $\Delta\theta_{SE}$  in the range of 0.61 to 0.67 degree, considerably larger than the rms value of  $\Delta\theta_{SE} = 0.24$  degree for the other 19 passes. Data from sun sensor 1 are assumed to be contaminated by a 0.6-degree misalignment<sup>15</sup>; thus, measurements from that sensor are not used to estimate sensor data accuracy.

The zero-mean rms noise on the measured sun and nadir vectors, assumed equal, is estimated to be  $\Delta\theta_{SE}/\sqrt{2} = 0.17$  degree. The rms error in the measured field direction, composed of zero mean and systematic errors, may be estimated by either  $\Delta\theta_{SM}$  or  $\Delta\theta_{EM}$ , reduced by the 0.17-degree rms error in the measured sun or nadir vector.\*\* These estimates are 0.31 degree and 0.47 degree, respectively, and are consistent with Equation (18) and the previous estimates of the field model accuracy cited in the introduction. Thus, we conclude that the inflight calibration of the HCMM magnetometers has removed most of the systematic measurement error, leaving only a systematic rms field model error of 0.25 to 0.5 degree and a zero-mean rms measurement error of 0.3 to 0.6 degree.

#### HCMM Yaw Determination Accuracy

The relationship among the residual rms errors,  $\Delta\theta_{SM}$  and  $\Delta\theta_{EM}$ , the rms error in the direction of the magnetic field, and errors in yaw derived from the calibrated magnetometer data are not easily shown analytically. These relations depend on the sensor accuracies and the reference vector geometry, given in Table 5 by the angles between the sun and magnetic field ( $\theta_{SM}$ ), and the angle between the nadir and magnetic field ( $\theta_{EM}$ ). The angle between the sun and the nadir ( $\theta_{SE}$ ) also is given in the table.

\*Attitude errors, however, may be smaller near the Equator because the nadir and field vectors are normal near the Equator and parallel near the poles.

\*\*The rms errors in the measured nadir and sun vector directions were previously estimated to be 0.17 degree and 0.20 degree, respectively, in Reference 6.

If we assume that the rms errors in the measurement of  $\hat{M}$  parallel and normal to  $\hat{E}$  are equal, then the rms yaw error is given by  $\Delta\theta_{EM}$  reduced by the error in the measurement of  $\hat{E}$ . If the 0.1 to 0.2 degree error in  $\hat{E}$  is neglected, then  $\Delta\theta_{EM}$  may be used as a conservative estimate of the rms yaw error. For the 43 passes composing the data base in Table 5,  $\Delta\theta_{EM}$  ranges from 0.32 to 0.96 degree, with an overall rms value of 0.53 degree.

Equation (11) with  $\sigma_B = 1.7$  mG,  $\sigma_\theta = 1.7$  degree, and

$$\hat{B}_0 = 230 \begin{bmatrix} \cos \lambda \\ 0 \\ 2 \sin \lambda \end{bmatrix} \text{ mG} \quad (20)$$

may also be used to estimate the systematic rms yaw angle errors.\* These results are shown in Table 6. Actual errors can be considerably larger because the spacecraft can pass much closer to the magnetic poles than indicated by the simple dipole field and the tracking station latitudes. The north magnetic pole is approximately 46 degrees of arc from Orroral Valley, Australia, and the south magnetic pole is about 25 degrees of arc from Fairbanks, Alaska.

Table 6 Typical RMS Yaw Errors Directly Over HCMM Tracking Stations Using a Dipole Field Model

STATION	LATITUDE	E LONGITUDE	RMS YAW ERROR ESTIMATE OVER TRACKING STATION (DEG)
ORR	26° 37'	142° 57'	0.57
MIL	25° 20'	179° 18'	0.52
GDS	20° 20'	243° 8'	0.97
ETC	20° 8'	282° 8'	0.62
MAD	42° 27'	128° 30'	0.83
WNE	51° 27'	228° 18'	0.88
ULA	64° 38'	172° 28'	1.24

Figure 3 compares sun sensor and magnetometer data yaw angle solutions over Winkfield, England, on November 29, 1978, at 11 hr 35 min GMT. The estimated rms error in the sun sensor yaw solutions is estimated by  $\Delta\theta_{SE}/\sqrt{2} = 0.17$  degree. (The angle between the sun and nadir ranged from 84 to 121 degrees during the pass and  $\Delta\theta_{SE} = 0.25$  degree.) The estimated rms error in the magnetometer yaw solutions is between the value of  $\Delta\theta_{EM} = 0.36$  degree and the value of 0.80 degree in Table 6. The mean of the two estimates,  $(0.36 + 0.80)/2 = 0.58$  degree, is shown as the error bar in the figure.

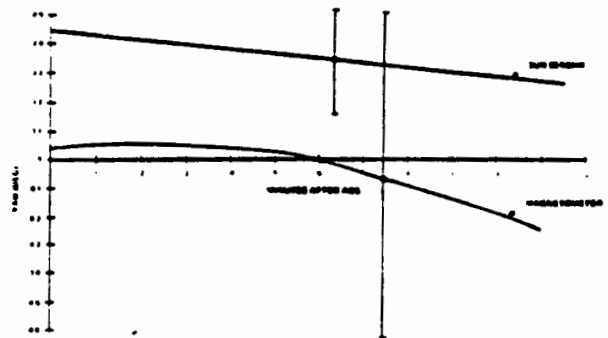


Fig. 3 Comparison of Sun Sensor and Magnetometer Yaw Angle Solution Over Winkfield

### Conclusions

An efficient and easily-implemented algorithm for the inflight calibration of magnetometers has been presented. The algorithm has been applied to Seasat-1 and AEM-1/HCMM flight data. For Seasat-1, large errors in the preflight calibration were computed, but a 3.7 mG residual, unmodeled bias on the data severely limited the obtainable yaw attitude accuracy. Inflight calibration of the HCMM magnetometers, however, removed large preflight calibration errors, including a 7 percent X-axis scale factor error, and enabled the use of magnetometer yaw data in support of HCMM experimental objectives. Errors in the geomagnetic field model were estimated and found to be 1 to 1.5 mG (rms) in magnitude and 0.5 degree (maximum) in direction, in agreement with earlier estimates at the HCMM, 600 km, altitude.

### Acknowledgment

The encouragement and support of Mr. Roger D. Working of the Attitude Determination and Control Section of NASA Goddard Space Flight Center is gratefully acknowledged.

### References

1. K. T. Alfriend, Magnetic Attitude Control System for Dual Spin Satellites, AIAA Journal, Vol. 13, June 1975
2. B. R. Leaton, International Geomagnetic Reference Field 1975, Transactions American Geophysical Union, Vol. 57, March 1976
3. G. F. Meyers, M. E. Plott, and D. E. Riggs, SAS-1 Data Analysis, NASA Goddard Space Flight Center, NASA X-542-71-363, August 1971
4. M. C. Phenneger, private communication

\* $\lambda$  is the subsatellite latitude when the spacecraft is traveling north, and 180 minus the latitude when the spacecraft is traveling south.

5. D. R. Sood, private communication
6. D. Niebur et al., Applications Explorer Mission-A/Heat Capacity Mapping Mission (AEM-A/HCMM) Post-Launch Report, Computer Sciences Corporation, CSC/TM-78/6221, September 1978
7. C. F. Manders et al., Seasat-1 Post-Launch Report, Computer Sciences Corporation, CSC/TR-79/6008 (in preparation)
8. M. C. Phenneger et al., Seasat-A Attitude System Functional Specifications and Requirements, Computer Sciences Corporation, CSC/SD-77/6001, March 1977
9. W. T. Nutt et al., Seasat-A Attitude Analysis and Support Plan, NASA Goddard Space Flight Center, NASA X-581-78-9, April 1978
10. B. T. Trombka and J. C. Cain, Computation of the IGRF, I. Spherical Expansions, Goddard Space Flight Center, NASA X-922-74-303, August 1974
11. K. Coriell, GEOS-3 Postlaunch Attitude Determination and Control Performance, Computer Sciences Corporation, CSC/TM-75/6149, August 1975
12. A. J. Treder, A Hybrid Technique for Spacecraft Attitude Interpolation With Arbitrary Attitude Data Gaps, Proceedings, Seventh Annual Conference on Modeling and Simulation, Pittsburgh, Pennsylvania, April 1977, published in William G. Vogt and Marlin H. Mickle, editors, Modeling and Simulation, Vol. 8, Instrument Society of American, 1977
13. D. Niebur et al., HCMM Attitude Analysis and Support Plan, NASA Goddard Space Flight Center, NASA X-581-78-4, March 1978
14. S. G. Hotovy, Evaluation of an Infrared Scanner Bias Determination Algorithm for Earth-Oriented Spacecraft, AAS/AIAA Astrodynamics Conference, Jackson Hole, Wyoming, September 7, 1977
15. D. Niebur, private communication